

Properties of Aqueous Solutions and Gels of Poly(ethylene oxide)-*b*-poly(propylene oxide)-*b*-poly(ethylene oxide)-*g*-poly(acrylic acid)

Lev Bromberg*

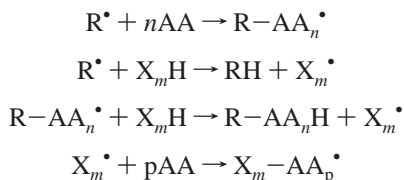
Department of Materials Science and Engineering, Massachusetts Institute of Technology, Cambridge, Massachusetts 02139

Received: July 24, 1998; In Final Form: October 14, 1998

Gelation in aqueous solutions of poly(acrylic acid) (PAA) grafted onto poly(ethylene oxide)-*b*-poly(propylene oxide)-*b*-poly(ethylene oxide) (Pluronic F127) has been studied. The gel point and onset of micellization are observed in Pluronic–PAA solutions at the same temperatures, confirming that the gelation occurs via formation of micelles that act as thermoreversible cross-links. The salt- and pH-dependent expansion or folding of the polyelectrolyte segments changes the gel elasticity. The increased polarity due to enhanced polymer ionization at higher pH or with salt addition causes the poly(propylene oxide) (PPO) segments to aggregate at lower temperatures. The weak dependence of the polymer concentration at the maximum reduced viscosity on the salt concentration is attributed to hydrophobic interactions among PPO segments.

Introduction

Hydrophobically modified polyelectrolytes (HMP) exhibit peculiar characteristics in aqueous solutions, such as an increase of solution viscosity upon salt addition (an “anti-polyelectrolyte effect”).^{1–3} The salt and pH effects on the rheological behavior of HMP originate from a delicate balance between the interchain aggregation due to hydrophobic interactions and the change in the coil dimensions because of the screening of electrostatic repulsion.¹ Among the most studied HMP are hydrophobically modified poly(acrylic acid) (HMPAA) and partially hydrolyzed polyacrylamides,⁴ as these polymers are readily available in a variety of molecular weights.^{5–11} Typically, HMPAA is synthesized by modification of PAA in its acidic form by alkylamines.^{1,6} The PAA–alkylamine coupling results in the attachment of oligomeric alkyl chains onto PAA backbone. The hydrocarbon of the same length as the group used for modification is water insoluble at any temperature. Thus, no large temperature effects on viscosity in these HMPAA have been reported. Recently, we have introduced a novel class of HMP whereby poly(propylene oxide) (PPO) group acts as a temperature-sensitive hydrophobe.^{12–23} Attachment of the PPO group onto a polyelectrolyte is a means of creating a dually responsive material by adding temperature-sensitivity to an already pH-sensitive polymer.¹² Synthetic scheme of these PEO–PPO–PEO–PAA copolymers involves free-radical polymerization of acrylic acid with the chain transfer to Pluronic resulting in grafting of PAA chains onto Pluronic backbone.¹⁴



where R^\bullet is the free radical,²⁰ X_mH is Pluronic, and AA is the acrylic acid monomer.

* To whom correspondence should be addressed: 15 Sherwood Road, Swampscott, MA 01907. E-mail: cpbrole@aol.com.

Efficiency of the grafting of PAA onto Pluronic backbone depends on grafting conditions, such as hydrogen abstraction power of the initiator, its concentration, etc.²⁰ Optimized synthetic procedure results in about 90% of Pluronic initially present in the reaction mixture being chemically bound to PAA.

Above certain temperatures, semidilute aqueous solutions of the PEO–PPO–PEO–PAA form gels with significant viscoelastic moduli.^{12,13}

The present study aimed at more detailed understanding of structure of the novel copolymers in aqueous solutions and mechanisms of their temperature-induced micellization. Rheological methods and differential scanning calorimetry revealed effects of pH and salt on the gelation.

Experimental Section

Materials. Pluronic F127 NF was kindly donated by BASF Corp. and used without further treatment. It has a formula $\text{EO}_{100}\text{PO}_{65}\text{EO}_{100}$, nominal molecular weight 12600, molecular weight of PPO segment 3780, 70 wt % of EO, and cloud point above 100 °C. Acrylic acid (99%), lauroyl peroxide (97%), benzoyl peroxide (97%), dodecane (99+%), and 2,2′-azobisisobutyronitrile (98%, AIBN) were purchased from Aldrich Chemical Co. and used as received. Initiators 2,2′-azobis(2,4-dimethylpentanenitrile) (Vazo 52) and 1,1′-azobiscyclohexanecarbonitrile (Vazo 88) were obtained from DuPont Specialty Chemicals (Wilmington, DE) and were recrystallized from cold acetone. Poly(vinylpyrrolidinone-*co*-1-hexadecene) (Ganex V-216) (dispersion stabilizer) was obtained from International Specialty Products and used as received. All other chemicals, gases, and organic solvents of the highest purity available were obtained from commercial sources.

Synthesis

Synthesis was carried out on a laboratory scale in an adiabatic mode. Poly(ethylene oxide)-*b*-poly(propylene oxide)-*b*-(poly(ethylene oxide))-*g*-poly(acrylic acid) (CAS no. 186810-81-1) was synthesized by dispersion/emulsion polymerization of acrylic acid along with simultaneous grafting of poly(acrylic

acid) onto the Pluronic backbone²⁰ as follows: Acrylic acid in a 125-mL flask was partially neutralized by addition of 50 w/w % aqueous NaOH solution while stirring. Degree of neutralization of acrylic acid was 6 mol %. Upon redissolution of the formed precipitate, Pluronic was charged into the flask and allowed to completely dissolve in acrylic acid under constant agitation. A 500-mL multinecked, thermostated flanged glass reactor equipped with a mechanical stirrer, syringe sampler, thermometer, programmable heater bath, and a gas inlet/outlet was charged with 400 mL of Ganex solution in dodecane and was deoxygenated overnight by nitrogen flow while stirring. The initiator system comprising a solution of lauroyl peroxide (140 mg) and 2,2'-azobis(2,4-dimethylpentanenitrile) (50 mg) in a small amount of acrylic acid was added into a solution of Pluronic (35 g) in partially neutralized acrylic acid (40 g). The resulting solution was deoxygenated by nitrogen flow for 1 h and introduced into the reactor under nitrogen blanket while stirring. The reactor was equilibrated for 1 h while stirring at 20 °C under nitrogen purge introduced from the bottom of the reactor. Then at $t = 0$ the heating began and timing commenced. The reactor was heated to 70 °C at a desired rate (typically 1–2 °C/min) under constant nitrogen flow. At a certain temperature the exothermic reaction began resulting in a rapid temperature rise inside the reactor. Then the heat release subsided and the reactor cooled to 70 °C and was kept at this temperature for 8–10 h under stirring. The reactor was allowed to equilibrate at 20 °C, the nitrogen flow was discontinued and the slurry of the resulting polymer was filtered off using Whatman filter paper (retention 10 μm). The polymer was repeatedly washed with excess heptane and then with excess hexane in separation funnels. The resultant white powder was dried under vacuum (10^{-3} Torr) at 40 °C for 24 h. Identical synthetic procedure (but without Pluronic) was used to synthesize poly(acrylic acid) (PAA).

Polymer Characterization Procedures

Size-exclusion chromatography (SEC) was run at various temperatures on a Shimadzu LC-10A Series HPLC set up with a Viscotek SEC³ triple detector system which included a laser scattering detector (scattering angle, 90°; wavelength, 670 nm; output power, 16 mW; cell volume, 12 μL), differential Wheatstone bridge viscometer (sensitivity, $1 \times 10^{-5} \eta_{\text{sp}}$; shear rate, 3000 s^{-1} ; cell volume, 50 μL), and a differential laser refractometer (wavelength, 670 nm; sensitivity, $3 \times 10^{-8} \Delta n$; shear rate, 3000 s^{-1} ; cell volume, 8 μL). A 0.01–1.0 mg/mL sample of polymer solution was loaded onto a Polymer Laboratories, Inc., aquagel-OH mixed, 40, and 60 analytical temperature-controlled 3-column system (particle size 8 or 15 μm ; dimensions 300 \times 7.5 mm, and then eluted using a selected buffer. The SEC system was calibrated in the MW range of 10^3 – 10^7 using poly(sodium acrylate) standards (American Polymer Standards Co.). For buffer preparation, ultrapure water from a Millipore Q purification system (conductivity less than 0.05 μS , outlet water filtered through a 0.22 μm filter) was utilized. Prior to use, polymer samples were dialyzed against excess buffer at 4 °C for 24 h with a Spectra/Por cellulose ester membrane (molecular weight cutoff 500). For fractionation, PL aquagel-OH 40 and 60 preparative columns (particle size 10 μm ; dimensions 300 \times 25 mm) were used. Buffers contained 50 or 100 mM Na_2HPO_4 and varying concentrations of NaNO_3 ; pH was adjusted to 7.0 by 1.0 M H_3PO_4 , as needed. To achieve optimum reliability of the SEC measurements, the effect of the Donnan salt exclusion was studied by varying NaNO_3 concentrations. The area of the salt peaks was minimized when ionic

strength of the buffer was 0.3 and 0.1 M for the PAA and Pluronic–PAA samples, respectively. This observation agrees well with reported optimum salt concentrations for PAA standards.²⁴

Rheological measurements within angular frequency (ω) range of 0.628 mrad/s to 628 rad/s (minimum strain 6×10^{-5}) were performed using a controlled stress Rheolyst Series AR1000 Rheometer (TA Instruments) with a cone and plate geometry system (cone: diameter, 4 cm; angle, 2°; truncation, 57 μm) equipped with a solvent trap. Temperature control (internal resolution 0.016 °C) was provided by two Peltier plates. Equilibrium flow experiments were conducted in a stepped ramp mode with the shear stress as a controlled variable. Oscillatory shear experiments were performed in both frequency and temperature ramp modes. Minimum strain and stress were 0.0143% and 6 mPa, respectively.

Viscometric titration was performed using a Cannon AutoVisc II automatic viscosity measuring system (Cannon Instrument Co.) equipped with a near-infrared optical sensor for meniscus detection and thermostatic air chamber for temperature control to within 0.01 °C.

Composition of the Pluronic–PAA copolymers was characterized by infrared spectroscopy. FTIR spectra were recorded in water-free atmosphere using a Nicolet Magna 550 IR System. Polymer powders were measured at 1 mg of polymer per 100 mg KBr containing 1 wt % KSCN as described elsewhere.^{14,23} Areas of the fitted Gaussian bands in the regions 1600–1800 cm^{-1} (COONa and COOH bands) and 1200–1000 cm^{-1} (ether bands of Pluronic) were averaged and compared to the area of the reference SCN Gaussian band centered at 2157 cm^{-1} . The ratio of the Gaussian peak areas was used to obtain the weight ratio of Pluronic and PAA components in the copolymer.

Calorimetry was run with a MC1 or MC2 differential scanning microcalorimeter (Microcal, Inc.) at a scanning rate of 1 °C/min. A distilled water reference was used and the water–water baseline was subtracted. The endotherm was normalized to the weight of the polymer.

Potentiometric titration was performed at 15 °C with 0.1 M NaOH using a Metrohm model 736 titration system equipped with a titration manipulator and a thermostat. The initial PAA and Pluronic–PAA concentration in solution was set at 70 mM acrylic acid units.

Results and Discussion

SEC Study. At low polymer concentrations, the SEC experiments resulted in chromatograms such as those shown in Figure 1. As can be seen, at 15 °C the chromatogram consisted of one peak that corresponded to nonaggregated species. Similar chromatograms were obtained in THF (data not shown).

As temperature increased, new peak(s), corresponding to higher molecular weights appeared and grew with temperature, so that the relative intensity of the fastest peak increased. It appears to be possible to follow entire aggregation process by varying the temperature (Figure 2).

Malmsten and Lindman²⁵ in their study of PEO–PPO–PEO block copolymers used analogous technique. The onset of aggregation in our SEC experiments at ~ 20 °C was independent of the flow rate. This result correlated well with the gelation threshold as described in the next chapter of this work.

Further SEC experiments provide some insight into conformation of the Pluronic–PAA copolymers, as compared to the PAA synthesized under similar conditions, but without the use of PEO–PPO–PEO copolymer as a chain transfer agent (Figure 3). While SEC of PAA was temperature independent within

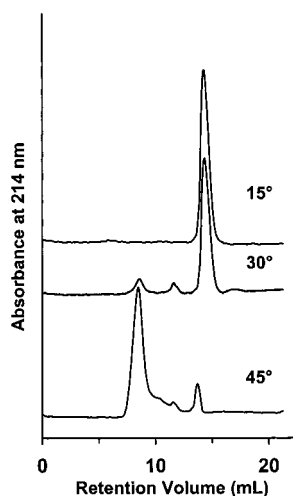


Figure 1. SEC chromatograms of Pluronic-PAA at different temperatures. The initial polymer concentration was 1 w/v %, solvent 0.1 M $\text{NaNO}_3/\text{Na}_2\text{HPO}_4$ (2:1 mole ratio, pH 7.0), flow rate 0.9 mL/min, injection volume 100 μL .

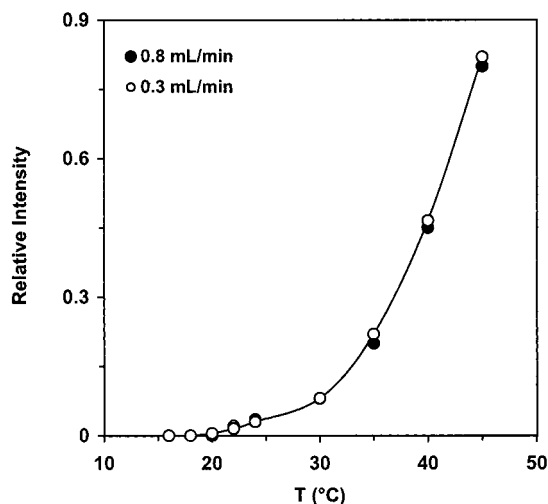


Figure 2. Temperature dependence of the relative intensity of the peak corresponding to the largest aggregates at different flow rates. For the run conditions, see Figure 1.

the range of 15–35 °C, the high molecular weight fraction of the light-scattering chromatograms of Pluronic-PAA was

sensitive to temperature (Figure 3B). The very high molecular weight peak did not disappear even at 15 °C. Since the viscometer did not respond to this peak, it had to have a very high density.

As aggregation can be ruled out at this temperature (compare with Figure 1 and data in ref 13), the high molecular weight peak indicates the presence of a small amount of cross-linked material.¹² To eliminate effects of permanent cross-linking in further analysis, fractions around the main peak were collected and separated as shown by arrows in Figure 3B. This resulted in a narrow molecular weight distribution of the Pluronic-PAA species (Figure 4).

Analogous fractionation technique applied to preparative SEC yielded sufficient amounts of Pluronic-PAA copolymers with polydispersity indexes not exceeding 2.1. These copolymers were used in the further study. Each polymer fraction was run at 15 °C in triplicate; the corresponding chromatograms were digitized, averaged, and analyzed in Mark-Houwink coordinates (Figure 5).

Lower a and K values found for the Pluronic-PAA than those for the corresponding PAA (Figure 5) indicate PAA modification and higher branching in the case of copolymer. Deviation from linearity in the $[\eta]$ vs M plots ascribed to the long-chain branching starts at $M_0 \approx 72\,000$ and $850\,000$ for PAA and Pluronic-PAA, respectively. It has been pointed out that free-radical polymerization of PAA with the $M > 10^6$ usually results in a branched polymer.^{24,29}

The value of the parameter a is meaningful from the polymer structure standpoint.²⁸ The θ -state for poly(sodium acrylate) has been observed at 15 °C and high salt concentration.^{24,30} In our experiments, PAA samples yielded $a = 0.499$ and $K = 1.5 \times 10^{-5}$ at 15 °C and $[\text{NaNO}_3] = 1.2$ M, in excellent agreement with the Mark-Houwink parameters for poly(sodium acrylate) at the θ -state.²⁴ However, aqueous buffers with moderate salt concentrations (0.3 M) and pH 7.0 may actually be good solvents for both PAA and Pluronic-PAA, provided that the temperature is below the onset of aggregation of the PPO segments in Pluronics. In these solvents, the a parameter for PAA was in the range $0.60 < a < 0.85$, indicating a random coil structure without significant expansion (no polyelectrolyte effect). The lower a values measured for all Pluronic-PAA samples to be in the range $0.48 < a < 0.59$ at 15 °C, along with the lower intrinsic viscosity to an equivalent molecular weight PAA suggest that the Pluronic-PAA samples possess

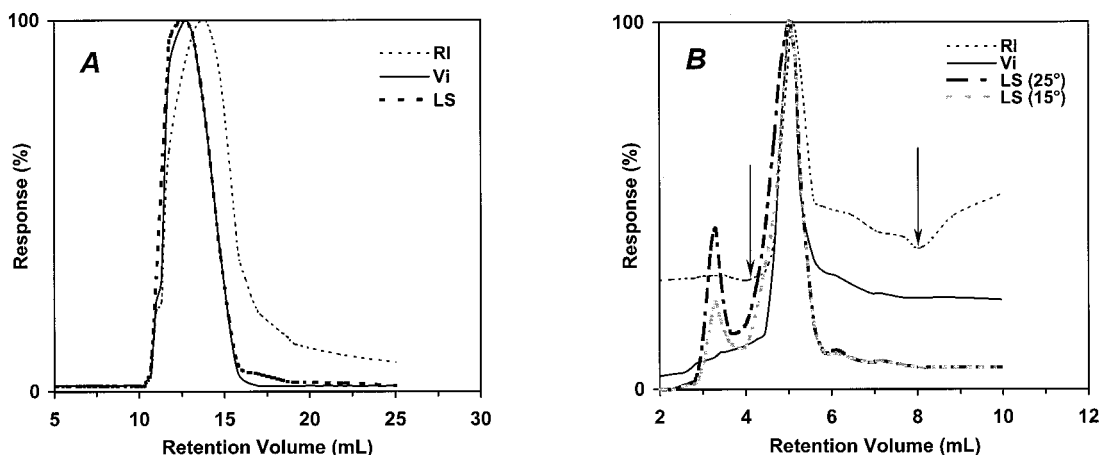


Figure 3. Triple-detector SEC chromatograms of (A) PAA and (B) Pluronic-PAA. In A, the initial polymer concentration was 0.1 w/v %, solvent 0.3 M $\text{NaNO}_3/\text{Na}_2\text{HPO}_4$ (1:1 mole ratio, pH 7.0), flow rate 0.8 mL/min, injection volume 100 μL , $T = 25$ °C; in B, the initial polymer concentration was 0.1 w/v %, solvent 0.1 M $\text{NaNO}_3/\text{Na}_2\text{HPO}_4$ (1:1 mole ratio, pH 7.0), flow rate 0.9 mL/min, injection volume 50 μL , $T = 15$ or 25 °C. LS, Vi, and RI stand for (normalized) outputs of the light scattering, differential viscometer, and refractive index detectors, respectively.

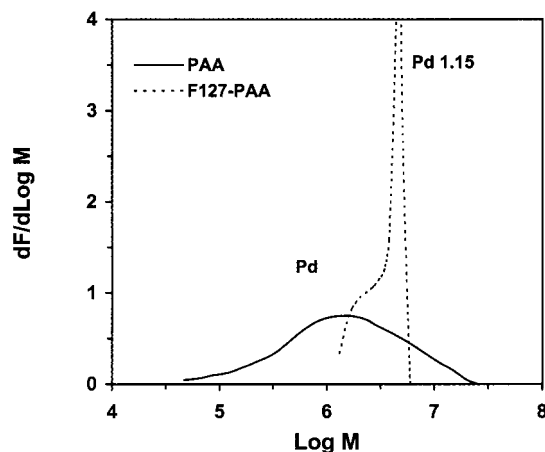


Figure 4. Differential molecular weight distributions of PAA and Pluronic–PAA samples shown in Figure 3.

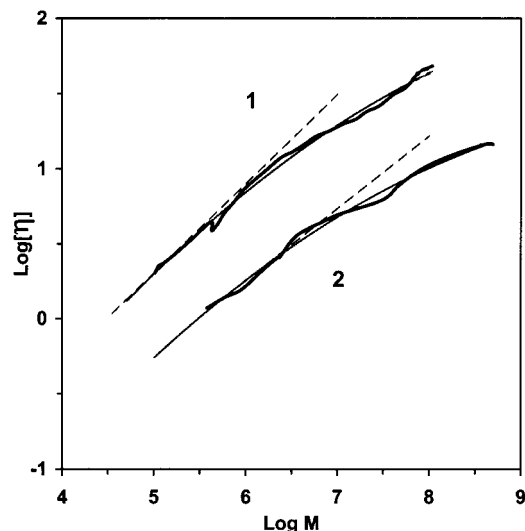


Figure 5. Intrinsic viscosity vs molecular weight plots of PAA and Pluronic–PAA samples. The data were approximated by the second-order polynomials $\log [\eta]_b = A(\log M)^2 + B \log M + C$, where M is the molecular weight and A , B , C are constants obtained from the best fit ($R^2 > 0.999$) to the experimentally found plot. The molecular weight corresponding to the start of long-chain branching ($M = M_0$) was calculated by minimizing equation $A(\log M)^2 + B \log M + C = \log K + a \log M$ with respect to M at the point where intrinsic viscosities of branched (dotted line) and linear (dashed line) flexible-chain polymers were equal ($[\eta]_b = [\eta]_l$). Here, constants a and K are parameters of the Mark–Houwink equation ($[\eta] = KM^a$).^{27,28} Number-, weight, z -average molar masses, and a values for PAA and Pluronic–PAA were 8.10×10^5 , 3.11×10^6 , 14.7×10^6 , and 0.60, and 3.13×10^6 , 3.61×10^6 , 3.99×10^6 , and 0.49, respectively.

higher molecular weight per repeat unit. This observation may be interpreted as a regular short-chain branching in Pluronic–PAA and is consistent with the synthetic mechanism, which involves chain transfer.^{14,23} The parameter a increased at lower added salt concentrations. For instance, $a = 1.21$ and 1.48 was observed in a 50 and 25 mM $\text{NaNO}_3/\text{Na}_2\text{HPO}_4$ buffer, respectively, at 15 °C. This indicates expansion of the Pluronic–PAA molecules. At the low-salt limit, a rodlike conformation is expected in the unentangled polyelectrolyte regime.³¹

Study of Gelation. SEC experiments discussed above (Figures 1 and 2) indicate the appearance of aggregates above certain temperature. However, since significant shear stresses are developed in our SEC system (see Experimental Section), the gelation point, strictly speaking, cannot be ascertained by SEC. To define the physical gelation threshold, we applied the

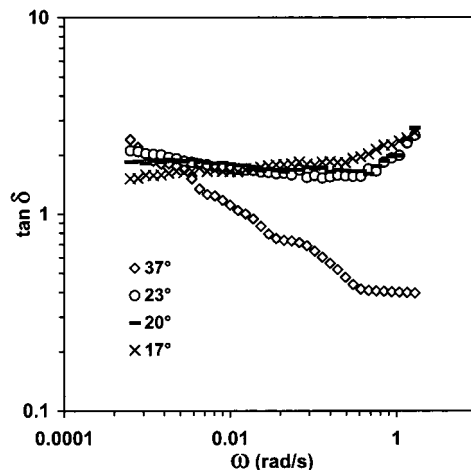


Figure 6. Temperature dependency of loss tangent of 1 w/v % Pluronic–PAA solution (pH 7.0) during frequency ramp. Oscillatory stress is 6 mPa.

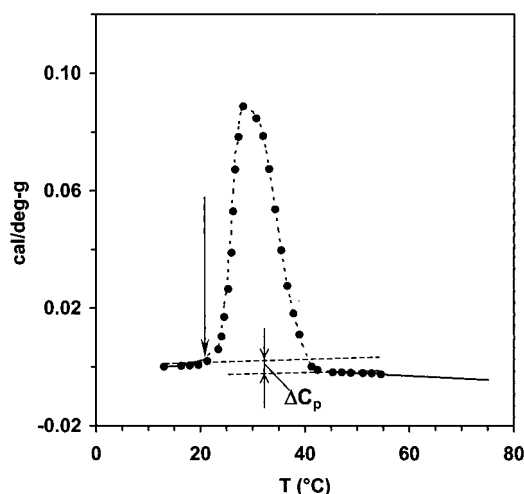


Figure 7. DSC output for 1 w/v % aqueous solution of Pluronic–PAA (pH 7.0) for the 1.0 K/min heating scan. Polymer fraction shown in Figure 5 was analyzed. Portion of the endotherm shown by the dashed line was model fitted as described in the Appendix A and the filled points represent each 10th of the computed data. Arrow shows critical micellization temperature; ΔC_p stands for the change in heat capacity.

Winter–Chambon method of detection of the diverging rheological properties.^{32–36} Namely, as dynamic mechanical properties of the system gradually evolve during the sol–gel transition, the gel point is reached when the loss tangent becomes independent of frequency:

$$\tan \delta_c = \frac{G_c''(\omega)}{G_c'(\omega)} = \tan \frac{\Delta\pi}{2} \quad \text{for} \quad 0 < \omega < 1/\tau_0,$$

$$p_{T_g, c_g} = p_c$$

where p is the degree of physical cross-linking, τ_0 is the characteristic relaxation time, and index c stands for the critical state at the gel point.

The instant of gelation was measured with the minimum modification of the molecular structure at lowest strains allowed by the instrument (Figure 6). Frequency-independent $\tan \delta$ was observed at 20 ± 3 °C, corroborating the observation that the onset of aggregation and the gel point (T_{gel}) in our system are close.¹² This conclusion is further supported by the DSC data analysis (Figure 7 and Appendix A).

It is significant to compare viscoelastic properties of the Pluronic–PAA solutions to the ones of Pluronic solutions and

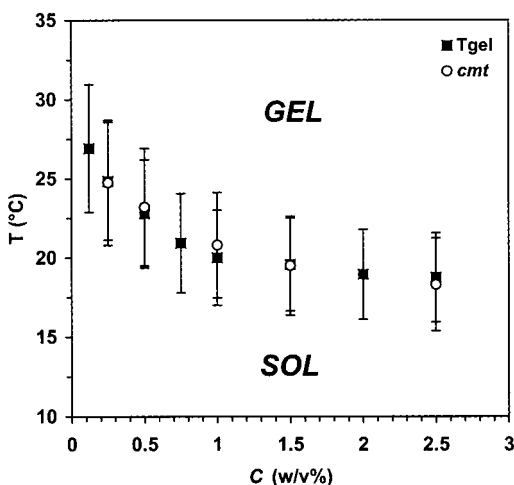


Figure 8. Phase diagram for aqueous solutions of Pluronic-PAA at pH 7.0. T_{gel} and cmt stand for the gel point and critical micellization temperatures determined by the Winter-Chambon method and DSC, respectively.

gels. Interestingly, no significant regions of frequency-independent $\tan \delta$ was observed in concentrated solutions of Pluronic F68 at any temperature, despite the formation of strong viscoelastic gels.³⁷ At elevated temperatures, Pluronic solutions yield gel networks consisting of interconnected micelles with entangled PEO segments.³⁸ In our case, gelation occurs due to aggregation of PPO segments, while the hydrophilic segments (PAA and PEO) remain unentangled.^{12,13} These differences in the mechanisms of gelation are probably accentuated by the differences in power law exponent Δ which was found to be 0.5 for Pluronic F68 gels³⁷ and $\Delta = 0.7$ in our experiments. The higher Δ may be explained by the aforementioned deficiency of the entanglements.³⁷ The Δ value observed in Pluronic-PAA aqueous solutions depends on the method of their synthesis.^{12,13,20} The polymers synthesized by the bulk polymerization yielded $\Delta = 0.5$,¹⁴ which is evidently related to the presence of permanent cross-linking and entanglements in this case. The dispersion polymerization utilized in the present study yields polymers with lesser degree of cross-linking.²⁰

The departure of the DSC signal from the model baseline can be defined as a critical micellization temperature (cmt).³⁹ The cmt coincidental with the gel point (Figure 8) confirms that

the appearance of micelles in our copolymer system is a cause of gelation. Correspondence between the experimental endotherm and the model fit (Figure 7) suggests relevance of the model (see Appendix A).

Relating the peak asymmetry to the changes in van't Hoff enthalpy (ΔH_{vH}) and consequently the ΔH_{vH} value with the average degree of aggregation n , we obtain $n = 6-18$ for the number of moles of unimeric chains per aggregate⁴⁰ in 1 w/v % solutions (data from 5 independent measurements). Defining unimers as the minimum-length copolymer chains containing single PPO segment capable of participation in a micelle, we obtain reasonable correlation with the average aggregation number of PPO segments in a core of the aggregate arrived at in the concurrent SANS study.^{17,19} Negative change in heat capacity (Figure 7) indicative of a decrease in the exposure of PPO segments to water⁴⁰ is consistent with the mechanism of micellization.⁴¹⁻⁴³

Effects of Salt and pH. Ionic strength and pH of an aqueous solution affect conformation of poly(acrylic acid)⁴⁴⁻⁴⁶ and influence micellization processes in Pluronic.⁴⁷ It was thus of interest to investigate how properties of the Pluronic-PAA copolymers depend on the presence of ions in their aqueous environment. Effects of pH on dynamic moduli of Pluronic-PAA solutions are shown in Figure 9. It can be seen that the onset of gelation (T_{gel}) that is reflected in the increase of the storage modulus shifted to lower temperatures with the increasing pH.

The strength of the gels formed above T_{gel} increased with the pH until certain extreme pH values (Figure 10). At pH > 11 the T_{gel} increased while the gels became less viscoelastic (Figures 9 and 10).

The observed changes in the elastic moduli can be explained by the progressive ionization of the PAA segments and increasing osmotic pressure inserted by the mobile counterions. When ionization is complete above pH 11 (Figure 11), the added NaOH electrostatically screens the charges on PAA and adds to the osmotic pressure of the solution surrounding the gel.¹⁰ Consequently, in the region of pH up to 12 the PAA segments expand with the increasing pH due to repulsive interactions between ionized carboxylic groups. Electrostatic screening at high pH leads to the transition of the PAA segments to the more compact state. Since the elasticity of our gels is directly proportional to the number of Pluronic-PAA chains connected

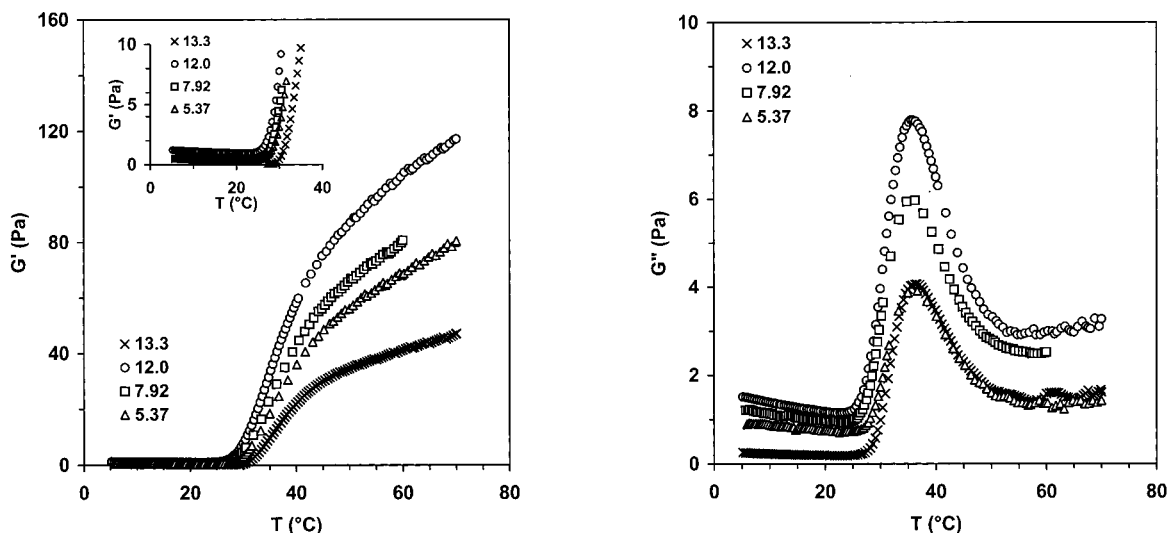


Figure 9. Effect of pH on temperature dependencies of storage (G') and loss (G'') moduli of 1 w/v % aqueous solutions of Pluronic-PAA. Numbers indicate pH. Frequency of oscillatory shear is 1 Hz, oscillatory stress 0.6 Pa, no salt added.

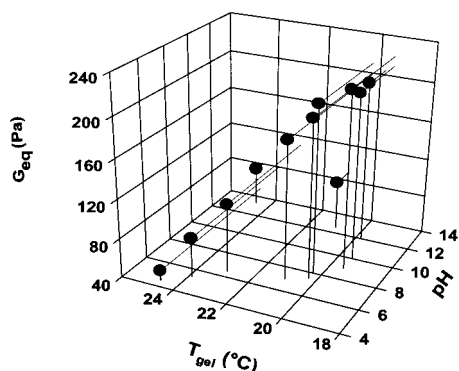


Figure 10. Effect of pH on the gel point (T_{gel}) and plateau modulus (G_{eq}) of 1 w/v % aqueous solutions of Pluronic–PAA. The T_{gel} values are measured by the Winter–Chambon method as described in the text. The G_{eq} values are determined from G' vs angular frequency plots at 37 °C at oscillatory stress of 6 mPa as previously described.¹²

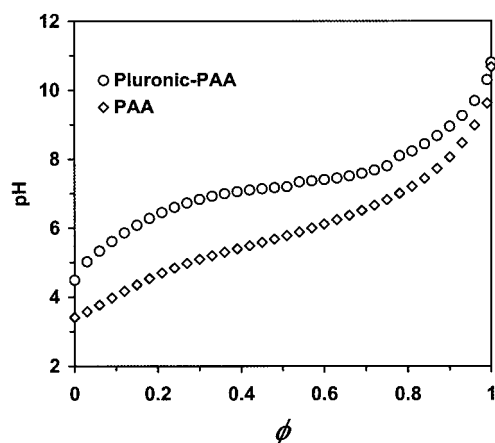


Figure 11. Potentiometric titration curves of aqueous solutions of Pluronic–PAA copolymer and PAA. The degree of ionization ϕ was computed as

$$\phi = \vartheta + \left(\frac{10^{pH}}{C_m} \right)$$

where ϑ is the degree of neutralization equal to the amount of NaOH required to completely neutralize all carboxylic groups in a sample and C_m is the concentration of acrylic acid units.

at both ends to the micelle-like aggregates,¹² the pH-dependent expansion or folding of PAA (which effects the chains' ability to participate in the aggregates) will increase or decrease, respectively, the gel elasticity. The increase in the PAA

ionization degree with pH will tend to turn the environment of the PPO segments more polar, hence driving the PPO segments to aggregate at lower temperatures (Figure 10). Screening of the ionization reverses this trend, increasing the T_{gel} values. It is interesting to observe that modification of the PAA with Pluronic lead to a shift of the ionization to higher pH in the resulting Pluronic–PAA copolymer, when compared to the PAA (Figure 11).

This phenomenon may be related to the formation of sterically constrained, hydrophobic domains of Pluronic onto which several PAA segments are attached.¹⁴ Such domains cause abrupt precipitation of the Pluronic–PAA in a narrow interval of $pH \leq 4.8$ when its basic solution is titrated with acid. No precipitation is observed with PAA under identical circumstances. Therefore, a higher pH is required to take the PAA segments in Pluronic–PAA apart making the carboxyl groups more accessible for the ionization. Analogous differences in the behaviors of PAA and poly(methacrylic acid) (PMAA) can be recalled.⁴⁶ While intrinsic viscosity (and thus the radius of gyration) of PAA increases with the charge density smoothly, the radius of gyration of PMAA coil does not increase until the charge density (reflecting repulsive force between coils) reaches a certain value. This is believed to be due to the hydrophobic interaction of the methyls in PMAA, which keeps the compact structure of the PMAA coils.⁴⁶

Effects of the salt addition on the properties of the Pluronic–PAA solutions are depicted in Figures 12 and 13. At low salt concentrations (about 10-fold lower than the acrylic acid concentration) the NaCl addition increases viscoelasticity in the solutions or gels due to the enhancement of hydrophobic interactions between the PPO segments.

At still higher salt concentrations, the electrostatic screening leads to the folding of the PAA segments, and the dynamic moduli and the cmt gradually decrease. The salt ions tend to compete with polyethers for the (structured) hydration water which is squeezed out to the bulk when two polymer chain approach each other closely.⁴⁹ The endothermic self-association between polyether chains becomes more thermodynamically favorable with the salt addition and will occur at lower temperatures.^{16,50} Analogous effects have been observed with other hydrophobically modified polyelectrolytes.³

When the salt concentration is fixed, the reduced viscosity (η_{sp}/C) of the Pluronic–PAA solutions (at temperatures below T_{gel}) exhibit concentration dependency (Figure 14) typical for

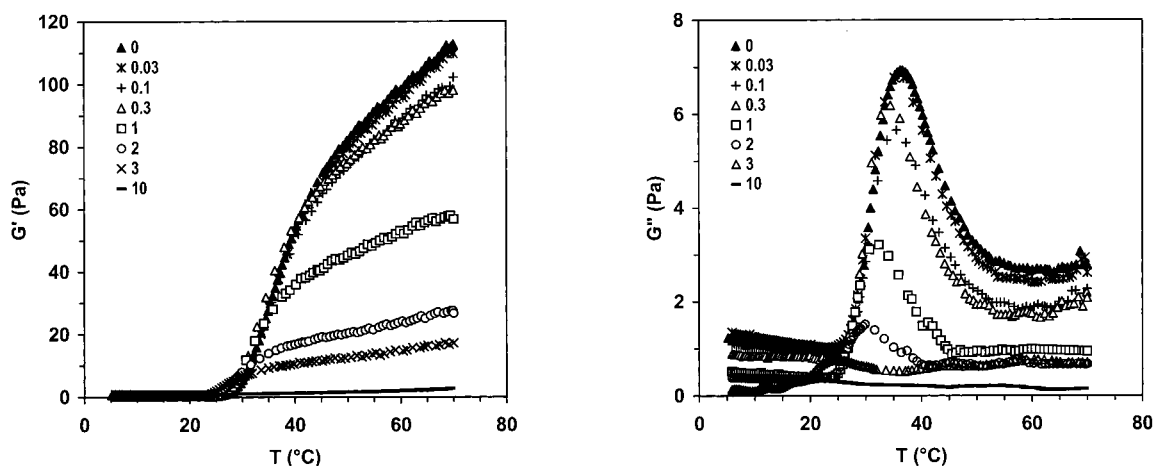


Figure 12. Effect of salt on temperature dependencies of storage (G') and loss (G'') moduli of 1 w/v % aqueous solutions of Pluronic–PAA. Numbers indicate w/v % NaCl concentrations. Frequency of oscillatory shear is 1 Hz, oscillatory stress 0.6 Pa, pH 7.0.

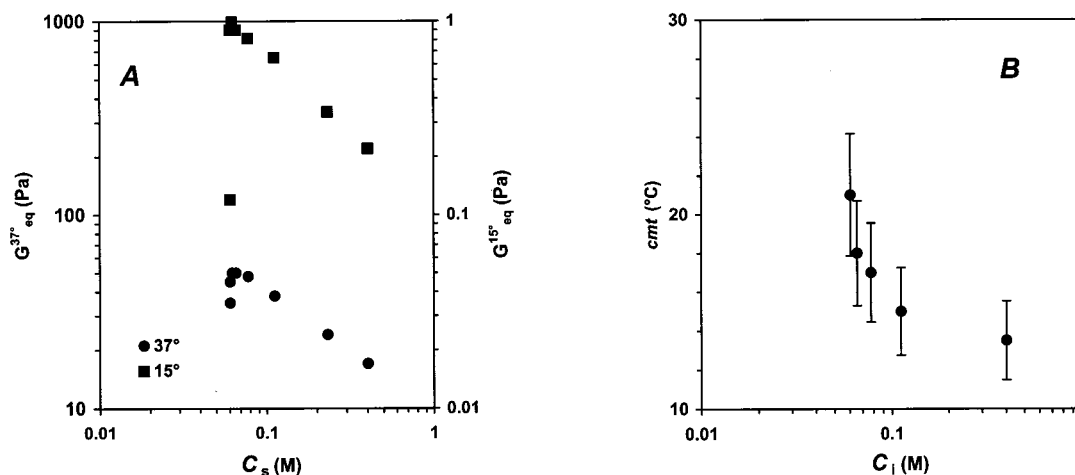


Figure 13. Dependencies of plateau moduli (G_{eq}) (A) and critical micellization temperature (cmt) (B) of 1 w/v % Pluronic-PAA on the total univalent electrolyte concentration (C_i). DSC as described in the text and Appendix A provided the cmt estimate. The C_i is obtained as ⁴⁸ $C_i = [\text{NaCl}] + C_p\tau/71$, where C_p is the total polymer concentration, $\tau = 0.425$ is the fractional ionization, and 71 is taken as the molecular weight per charge group.

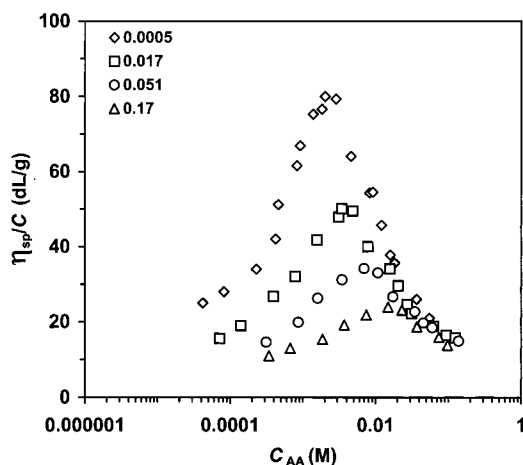


Figure 14. Reduced viscosity of Pluronic-PAA aqueous solutions (pH 7.0) at 15 $^\circ\text{C}$ as a function of molar concentration of acrylic acid units (C_m). Numbers indicate concentration of NaCl added (mol/L). Polymer fraction is used that is described in Figure 5.

polyelectrolytes.^{51–54} The reduced viscosity shows a pronounced maximum at a monomer concentration C_m^{\max} that depends on the salt concentration. The nature of such maximum can be explained by counterion condensation (Appendix B). The value of $(\eta_{sp}/C)_{\max}$ and the position of the corresponding C_m^{\max} depend on salt concentration (Figure 14). Importantly, a much weaker dependence of C_m^{\max} on C_s was observed with Pluronic-PAA than in the case of a strong polyelectrolyte with a hydrophobic backbone, poly(sodium styrene sulfonate) (PSS).⁵¹ With PSS, the slope of the C_p vs C_s plot was observed to be 4.0.⁵¹ Clearly the weak dependence of C_m^{\max} on C_s is due to “anomalous” effect of C_s on viscosity (compare with Figure 12). Dependence of $[\eta] \sim C_s^{-0.5}$ is well-known for linear polyelectrolytes, whereas hydrophobically modified polyelectrolytes show much more complex dependencies due to intra- and intercoil hydrophobic interactions.^{1,4}

Most conformation-based models developed for polyelectrolytes^{55–58} predict that a maximum in reduced viscosity occurs when the salt and the counterion concentration are of the same order of magnitude. We, however, observe significant deviations from the predicted correlation (Figure 14). The curves in Figure 14 coalesce at about $C_m = 0.02$ M which is about an order of magnitude higher than the value of critical concentration C^{**}

predicted by Odijk.⁵⁹ The C^{**} is associated with the melting of so-called polyion lattice⁵⁵ when the electrostatic persistence length becomes comparable to the correlation length (assuming semidilute regime). Future studies should reveal the meaningfulness of this comparison. It is believed that sufficiently detailed theory of the hydrophobically modified polyelectrolytes is lacking at present.

Conclusions

Poly(acrylic acid) (PAA) was grafted onto poly(ethylene oxide)-*b*-poly(propylene oxide)-*b*-poly(ethylene oxide) (Pluronic F127) by a one-step dispersion polymerization procedure to result in a temperature-gelling copolymer (Pluronic-PAA). Aggregation process in aqueous solutions of Pluronic-PAA was followed in SEC experiments by varying the temperature. The onset of aggregation was observed at ~ 20 $^\circ\text{C}$ and was independent of the flow rate. Pluronic-PAA samples possess higher than PAA molecular weight per repeat unit which is indicative of a regular short-chain branching in Pluronic-PAA and is consistent with the synthetic mechanism involving chain transfer to Pluronic.¹⁴ Neighboring onset of micellization and the gel point (T_{gel}) at 20 ± 3 $^\circ\text{C}$ were observed in 1 w/v % Pluronic-PAA solutions by frequency-independent $\tan \delta$ and DSC, confirming that the gelation occurs via micellization. Here, the micelles act as thermoreversible cross-links. Negative change in heat capacity upon gelation suggests a decrease in the exposure of poly(propylene oxide) segments to water and is consistent with the formation of micelles. As the gel elasticity is directly proportional to the number of Pluronic-PAA chains connected at both ends to the micelles, the pH-dependent expansion or folding of PAA (which effects the chains' ability to participate in the aggregates) alters the gel elasticity. As the polymer ionization increases with pH or salt addition, the environment of the PPO segments becomes more polar. The increased polarity forces the PPO segments to aggregate at lower temperatures. Conversely, screening of the ionization increases the T_{gel} values. The reduced viscosity of the Pluronic-PAA solutions shows a pronounced maximum at a polymer concentration that depends on the salt concentration. The appearance of such maximum is due to the counterion condensation. The weak dependence of the polymer concentration at the maximum reduced viscosity on the salt concentration is attributed to intra- and intercoil hydrophobic interactions between PPO segments.

Appendix A

Our DSC analysis originates from the two-state model of an association-dissociation process⁶⁰ and is analogous to the one recently described.^{40,60} Namely, aggregation in our copolymer system is considered as a process whereby n monomeric molecules A reversibly form an aggregate:



where K is the equilibrium constant.

Combining definition of the equilibrium constant and the mass action law, one obtains

$$K = \frac{[A_n]}{[A]^n} = \frac{\alpha}{n(1-\alpha)^n C^{n-1}} \quad (\text{A-2})$$

where α is the extent of aggregation and C is the total polymer concentration.

Assuming the enthalpy change to be independent of temperature,⁶⁰ the integral form of the van't Hoff isochore can be related to K :

$$\ln K = \frac{-\Delta H_{\text{vH}}}{RT} + \text{const} \quad (\text{A-3})$$

where ΔH_{vH} , R , and T are the van't Hoff enthalpy, gas constant, and absolute temperature, respectively. The integration constant in eq A-3 is traditionally found by setting $T = T_{0.5}$ at $\alpha = 0.5$.

Since the output of the DSC instrument is actually a power (W) needed to balance changing temperatures in the sample and reference cells,⁶¹ the W is related to the excess heat capacity of the sample ΔC_p . Hence,

$$\Delta C_p = \frac{W}{rN} = \Delta H_{\text{DSC}} \frac{d\alpha}{dT} \quad (\text{A-4})$$

where r is the scan rate and ΔH_{DSC} is the area under the DSC curve.

The derivative $d\alpha/dT$ is obtained from eq A-2 and A-3

$$\frac{d\alpha}{dT} = \frac{\Delta H_{\text{vH}}}{RT^2} \left(\frac{1}{\alpha} + \frac{n}{1-\alpha} \right)^{-1} \quad (\text{A-5})$$

The latter equation was used in our computation procedure to convert the DSC output into a function of α vs T . The α value was approximated by the ratio of the enthalpy released at given temperature to the total enthalpy change in the process. A least-squares fitting was used to find the best-fit values for n and $T_{0.5}$.

Appendix B

The concept of counterion condensation is instituted by Manning.⁶² Namely, the degree of ionization of PAA chains increases with salt concentration until a certain critical value (ϕ_c) after which the salt and the polyion counterions (Cl^- and H^+ , respectively) “condense”. Above ϕ_c , the polymer's charge density (ξ) decreases with polymer concentration. The ξ is given by⁵²

$$\xi = \frac{l_B}{d} \quad (\text{B-1})$$

where l_B is the Bjerrum length and d is the linear distance between separated charges along the polymer chain.

The inverse Debye screening length $k = \xi^{-1}$ can be presented as⁶³

$$k^2 = k_s^2 + k_p^2; k_s^2 \propto \Psi_s; k_p^2 \propto \Psi_p \quad (\text{B-2})$$

where Ψ is the molar concentration of the (ionizable) monomer or salt and indexes p and s stand for polymer counterions and salt ions, respectively.

Thus in the region $\phi > \phi_c$ ($C_m > C_m$) the k_p that results from free counterions is nearly constant. Following the $\phi = \phi_c$ point, upon dilution the counterions are “bound” and are less osmotically active, resulting in the decrease of k_p . On the other hand, the free salt contribution k_s increases throughout the concentration range. From these trends, the inverse Debye lengths at high and low concentrations can be compared (eqs B-1 and B-2). As k_p and k_s dominate regions $C_m > C_m^{\text{max}}$ and $C_m < C_m^{\text{max}}$, respectively, the net k will have a minimum at $C_m = C_m^{\text{max}}$.⁵² Since to a first approximation the reduced viscosity is reciprocally proportional to k^3 , a maximum on the η_{sp}/C versus C_m plot is observed at $C_m = C_m^{\text{max}}$.

References and Notes

- (1) Magny, B.; Iliopoulos, I.; Audebert, R. In *Macromolecular Complexes in Chemistry and Biology*; Dubin, P., Bock, J., Davis, R., Schulz, D. N., Eds.; Springer: Berlin, 1994; Chapter 4.
- (2) Magny, B.; Lafuma, F.; Iliopoulos, I. *Polymer* **1992**, *33*, 3151.
- (3) Wang, T. K.; Iliopoulos, I.; Audebert, R. In *Water-Soluble Polymers*; Shalaby, S. W., McCormick, C. L., Butler, G. B., Eds. ACS Symposium Series 467, American Chemical Society: Washington, DC, 1991; Chapter 14.
- (4) Bock, J.; Varadaraj, R.; Schulz, D. N.; Maurer, J. J. In *Macromolecular Complexes in Chemistry and Biology*; Dubin, P., Bock, J., Davis, R., Schulz, D. N., Eds.; Springer: Berlin, 1994; Chapter 3.
- (5) Bokias, G.; Hourdet, D.; Iliopoulos, I.; Staikos, G.; Audebert, R. *Macromolecules* **1997**, *30*, 8293.
- (6) Wang, T. K.; Iliopoulos, I.; Audebert, R. *Polym. Bull.* **1988**, *20*, 577.
- (7) Petit, F.; Audebert, R.; Iliopoulos, I. *Colloid Polym. Sci.* **1995**, *273*, 777.
- (8) Bokias, G.; Hourdet, D.; Iliopoulos, I.; Staikos, G.; Audebert, R. *Macromolecules* **1997**, *30*, 8293.
- (9) Tribet, C.; Porcar, I.; Bonnefont, P. A.; Audebert, R. *J. Phys. Chem. B* **1998**, *102*, 1327.
- (10) Philippova, O. E.; Hourdet, D.; Audebert, R.; Khokhlov, A. R. *Macromolecules* **1997**, *30*, 8278.
- (11) Philippova, O. E.; Hourdet, D.; Audebert, R.; Khokhlov, A. R. *Macromolecules* **1996**, *29*, 2822.
- (12) Bromberg, L. *Langmuir* **1998**, *14*, 5806.
- (13) Bromberg, L. *Macromolecules* **1998**, *31*, 6148.
- (14) Bromberg, L. *J. Phys. Chem. B* **1998**, *102*, 1956.
- (15) Bromberg, L.; Lupton, E. C.; Schiller, M. E.; Timm, M. J.; McKinney, G. W.; Orkisz, M. Hand. B. Int. Pat. Appl. WO 97/00275, 1997.
- (16) Bromberg, L. E.; Ron, E. S. *Adv. Drug Delivery Rev.* **1998**, *31*, 197.
- (17) Huibers, P. D. T.; Lupton, E. C.; Bromberg, L. E.; Hatton, T. A. In *Supplement to Chemical and Engineering Progress, Annual Meeting of the American Institute of Chemical Engineers*; Los Angeles, 1997; paper 93c.
- (18) Bromberg, L.; Orkisz, M.; Roos, E.; Ron, E. S.; Schiller, M. J. *Controlled Release* **1997**, *48*, 305.
- (19) Huibers, P. D. T.; Bromberg, L. E.; Lupton, E. C.; Hatton, T. A. Manuscript in preparation.
- (20) Bromberg, L. *Ind. Eng. Chem. Res.* **1998**, *37*, 4267.
- (21) Bromberg, L. *Polymer* **1998**, *39*, 5663.
- (22) Bromberg, L. E.; Mendum, T. H. E.; Orkisz, M. J.; Ron, E. S.; Lupton, E. S. *Proc. Polym. Mater. Sci. Eng.* **1997**, *76*, 273.
- (23) Bromberg, L. *Macromol. Rapid Commun.* **1998**, *19*, 467.
- (24) Kato, T.; Tokuya, T.; Nozaki, T.; Takahashi, A. *Polymer* **1984**, *25*, 218.
- (25) Malmsten, M.; Lindman, B. *Macromolecules* **1992**, *25*, 5440.
- (26) Vilenchik, L.; Ayotte, R. *J. Appl. Polym. Sci.: Appl. Polym. Symp.* **1992**, *51*, 73.
- (27) Cooper, A. R. In *Polymers: Polymer Characterization and Analysis*; Kroschwitz, J. I., Ed.; Wiley: New York, 1990; p 481.
- (28) Yamakawa, H. *Modern Theory of Polymer Solutions*; Harper and Row: New York, 1971.

- (29) Kawaguchi, S.; Takahashi, T.; Tajima, H.; Hirose, Y.; Ito, K. *Polym. J.* **1996**, *28*, 735.
- (30) Takahashi, A.; Nagasawa, M. *J. Am. Chem. Soc.* **1964**, *86*, 543.
- (31) Dobrynin, A. V.; Colby, R. H.; Rubinstein, M. *Macromolecules* **1995**, *28*, 1859.
- (32) Chambon, F.; Winter, H. H. *Polym. Bull.* **1985**, *13*, 499.
- (33) Schwittay, C.; Mours, M.; Winter, H. H. *Faraday Discuss.* **1995**, *101*, 93.
- (34) Winter, H. H. *Prog. Colloid Polym. Sci.* **1987**, *71*, 104.
- (35) Mours, M.; Winter, H. H. *Macromolecules* **1996**, *29*, 7221.
- (36) Winter, H. H.; Mours, M. *Adv. Polym. Sci.* **1997**, *134*, 165.
- (37) Nyström, B.; Walderhaug, H. *J. Phys. Chem.* **1996**, *100*, 5433.
- (38) Mortensen, K.; Brown, W.; Jørgensen, E. *Macromolecules* **1994**, *27*, 5654; **1995**, *28*, 1458.
- (39) Yu, G.-E.; Deng, Y.; Dalton, S.; Wang, Q.-C.; Attwood, D.; Price, C.; Booth, C. *J. Chem. Soc., Faraday Trans.* **1992**, *88*, 2537.
- (40) Paterson, I.; Armstrong, J.; Chowdry, B.; Leharne, S. *Langmuir* **1997**, *13*, 2219.
- (41) Linse, P.; Malmsten, M. *Macromolecules* **1992**, *25*, 5434.
- (42) Linse, P. *Macromolecules* **1993**, *26*, 4437.
- (43) Linse, P. *J. Phys. Chem.* **1993**, *97*, 13896.
- (44) Yin, Y.-L.; Prud'homme, R. K.; Stanley, F. In *Polyelectrolyte Gels*; Harland, R. S., Prud'homme, R. K., Eds.; ACS Symposium Series 480, American Chemical Society, Washington, DC, 1992; Chapter 6.
- (45) Buchholz, F. L. In *Modern Superabsorbent Polymer Technology*; Buchholz, F. L., Graham, A. T., Eds.; Wiley: New York, 1998; Chapter 5.
- (46) Noda, I.; Tsuge, T.; Nagasawa, M. *J. Phys. Chem.* **1970**, *74*, 710.
- (47) Alexandridis, P.; Hatton, T. A. *Colloids Surf. A* **1995**, *96*, 1.
- (48) Reed, W. F.; Ghosh, S.; Medjahdi, G.; François, J. *Macromolecules* **1991**, *24*, 6189.
- (49) Gombotz, W. R.; Guanghui, W.; Horbett, Hoffman, A. S. In *Poly(ethylene Glycol) Chemistry. Biotechnical and Biomedical Applications*; Harris, J. M., Ed.; Plenum Press: New York, 1992; pp 247–261. Antonsen, K. P.; Hoffman, A. S. In *Poly(ethylene Glycol) Chemistry. Biotechnical and Biomedical Applications*; Harris, J. M., Ed.; Plenum Press: New York, 1992; pp 15–28.
- (50) Armstrong, J. K.; Chowdhry, B.; Showden, M. J.; Leharne, S. A. *Langmuir* **1998**, *14*, 2004.
- (51) Cohen, J.; Priel, Z.; Rabin, Y. *J. Chem. Phys.* **1988**, *88*, 7111.
- (52) Hodgson, D. F.; Amis, E. J. *J. Chem. Phys.* **1989**, *91*, 2635.
- (53) Hodgson, D. F.; Amis, E. J. *J. Chem. Phys.* **1991**, *94*, 4581.
- (54) Vink, H. *J. Chem. Soc., Faraday Trans.* **1987**, *83*, 801.
- (55) de Gennes, P. G.; Pincus, P.; Velasco, R. M.; Brochard, F. *J. Phys. (Paris)* **1976**, *37*, 1461.
- (56) Reed, W. F. *J. Chem. Phys.* **1994**, *101*, 2515.
- (57) Rubinstein, M.; Colby, R. H.; Dobrynin, A. V. *Phys. Rev. Lett.* **1994**, *73*, 2776.
- (58) Barrat, J.-L.; Joanny, J.-F. In *Advances in Chemical Physics*; Prigogine, I., Rice, S. A., Eds.; 1996; Vol. XCIV, Chapter 1.
- (59) Odijk, T. *Macromolecules* **1979**, *12*, 688.
- (60) Freire, E. *Comments Mol. Cell. Biophys.* **1989**, *6*, 123.
- (61) Armstrong, J.; Chowdhry, B.; Mitchell, J.; Beezer, A.; Leharne, S. *J. Phys. Chem.* **1996**, *100*, 1738.
- (62) Privalov, P. L.; Potekhin, S. A. *Methods Enzymol.* **1986**, *131*, 4.
- (63) Manning, G. S. *J. Chem. Phys.* **1969**, *51*, 924.
- (64) Eisenberg, H. *Biological Macromolecules and Polyelectrolytes in Solution*; Oxford University: London, 1976.